Earth Planets Space, **59**, 279–285, 2007

Analysis of ionospheric scintillation spectra and TEC in the Chinese low latitude region

Guozhu Li[1,2,3], Baiqi Ning[1], and Hong Yuan[4]

[1]*Institute of Geology and Geophysics, Chinese Academy of Sciences, Beijing, China*
[2]*Wuhan Institute of Physics and Mathematics, Chinese Academy of Sciences, Wuhan, China*
[3]*Graduate School of Chinese Academy of Sciences, Beijing, China*
[4]*Academy of Opto-electronics, Chinese Academy of Sciences, Beijing, China*

(Received November 29, 2005; Revised November 23, 2006; Accepted November 23, 2006; Online published May 7, 2007)

GPS L-band scintillations and total electron content (TEC) were recorded at Sanya (18.33°N, 109.52°E) during the period July 2004–July 2005. Automatic recorded raw digital scintillation data are analyzed to obtain the spectral characteristics of irregularities producing ionospheric scintillations and to estimate the correlation between amplitude scintillation and power spectral density. Concurrent measurements of TEC are used to analyze ROTI, defined as the standard deviation of the rate of change of TEC. The statistical results of S4 indices and power spectral indices indicate that the power spectral indices increase with S4 indices for weak scintillation ($0.1 \leq S4 < 0.3$), but for moderate and strong scintillation, spectral indices tend to be saturated. In the analyzed data set, the ratio of ROTI/S4 is found to vary between 0.3 and 6, and the variation in estimated zonal drift velocities during geomagnetic quiet days ($Kp < 3$) shows that the motion of the irregularities is highly variable in the initial phase of irregularity development. After about 22:00 LT, the estimated drift velocities tend to follow the same pattern.

Key words: GPS TEC, scintillation spectra, ionospheric irregularities.

1. Introduction

Ionospheric scintillation is a relatively rapid fluctuation of the amplitude phase of the radio signal and is mostly caused by irregularities in the ionospheric electron density along the path that the signal propagated. The percentage of irregularities in these fluctuations is usually very small, but it can be as large as nearly 100% near the equator (Basu and Khan, 1976). The irregularities are predominantly in the F-layer of the ionosphere at altitudes ranging from 200 to 1000 km, with the primary disturbance region being typically between 250 and 400 km. It is well established that the large-scale plasma depletions are generated first in the post-sunset period through the Rayleigh-Taylor instability and that the depleted regions rise quickly to cover the entire F-region, including the topside ionosphere. Plasma processes then give rise to instabilities acting on the steep gradients available and generate smaller and smaller scale sizes in a cascade process (Haerendel, 1973). The generated plasma bubbles have typical east-west dimensions of several hundred kilometers, and they contain irregularities with scale-lengths ranging from tens of kilometers to tens of centimeters (Woodman and LaHoz, 1976). Basu *et al*. (1978) showed that between sunset and midnight, 3-m scale irregularities that cause radar backscatter at 50 MHz, co-exist with sub-kilometer scale irregularities that cause L-band scintillations.

The trans-ionospheric signal scintillation causes considerable communication hazards at a wide range of frequencies and is therefore of great practical interest (Banerjee *et al*., 1992). Since ionospheric scintillation originates from random electron density irregularities acting as wave scatters, research on the formation and evolution of these irregularities is closely related to the scintillation studies.

Over the past two decades, many excellent reviews of scintillation theory and observations have been published (e.g., Aarons, 1982, 1993; Yeh and Liu, 1982; Basu and Basu, 1985, 1993; Bhattacharyya and Rastogi, 1985, 1991; Bhattacharyya *et al*., 1990, 1992). Comprehensive reviews of the physics of ionospheric irregularities can also be found in many articles (e.g., Keskinen and Ossakow, 1983; Heppner *et al*., 1993; Fejer, 1996). Recently, Aarons *et al*. (1996, 1997) utilized GPS data to study ionospheric irregularities of electron density. Pi *et al*. (1997) have defined a ROTI index, based on the standard deviation of the rate of change of total electron content (TEC) over a 5-min period. By comparing amplitude scintillations (S4) with TEC fluctuations, Beach and Kintner (1999) concluded that the S4 index is roughly proportional to the measures of TEC fluctuation for weak scintillation and that the ratio ROTI/S4 varies between 2 to 5. Using their own data set, Basu *et al*. (1999) similarly found that ROTI/S4 varies between 2 to 10.

Most observations of scintillation have been carried out close to the magnetic equator in African, American and Indian sectors (Taur, 1973; Chandra *et al*., 1979; Aarons, 1982; Rastogi, 1982; Rastogi *et al*., 1982; Basu and Basu, 1985; Pathan *et al*., 1991). In order to study temporal and

spatial variations of ionospheric scintillation in the Chinese low latitude region, a GPS ionospheric scintillation receiver was established at Sanya (18.33°N, 109.52°E) in June 2004 to record scintillations at the L1 band. Employing the ROTI value, S4 index and estimated irregularity spectral index as the means of analyzing the TEC fluctuations, we have studied the spectral characteristics and transverse drift velocities of the scintillation-producing irregularities, the evolution of large- and small-scale irregularities associated with scintillation, and the variability of their motion.

2. Observations and Analytical Process

Ionospheric scintillation measurement was performed using the GPS Ionospheric Scintillation/TEC Monitor (GISTM), model GSV4004 (Van Dierendonck *et al.*, 1993). The system is NovAtel's Euro4 dual-frequency receiver version of the OEM4 card with special firmware, which was especially developed to maintain lock even under strong scintillation conditions. The scintillation monitor uses a semi-codeless technique to extract the GPS L2 signal, and the PLL (phase lock loop) tracking loops have a bandwidth (10 Hz) that has been optimally chosen to overcome scintillation effects. In order to keep the raw digital scintillation data for our detailed spectral analysis off line, we have developed a new control and processing software based on the GISTM to automatically keep the raw digital data (50 Hz) when scintillation occurs, including 10 min of raw digital data before and after the scintillation event (Li et al., 2005).

We have used the widely known amplitude scintillation index S4 to estimate the intensity of the observed scintillation. The S4 index is defined as the standard deviation of the received signal power normalized to the average signal power (Briggs and Parkin, 1963). It is calculated for each 1-min period based on a 50-Hz sampling rate (3000 data samples). The GISTM also computes the S4 index due to ambient noise in such a way that a corrected S4 index (without noise effects) can be computed (Van Dierendonck *et al.*, 1993). The corrected S4 index is used in the following analyses.

As the ionospheric irregularities drift across the path of the radio signal, the spatial pattern of varying intensity is converted into temporal fluctuations or scintillations and recorded by the ground receiver. Parameters such as height and thickness of the irregularity, strength of the density fluctuations, background plasma density, irregularities in the power spectrum, among others determine the S4 index and the distribution of the spatial scale lengths in the ground scintillation pattern. Therefore, the power spectra of the scintillation event contain information about the irregularities that produce the scintillation. Here, the power spectrum is computed for each 1-min period of the raw data, with 0.02 s of sampling, via Fast Fourier Transform (FFT) using the standard software routine. The power spectral analysis of scintillation has a confidence level $\geq$0.95.

The standard deviation of ROT (the rate of change of TEC), defined as ROTI, is computed over 5-min intervals (Pi *et al.*, 1997). TEC data for ROTI measures are also obtained from GISTM. In the data processing procedure, ROT is computed for each 30-s interval and converted to the unit of TECU/min. Since observations at lower elevation angles have passed through a longer path through the ionosphere than those at high elevation angles, the slant TEC values were approximated into the equivalent vertical TEC values by assuming a thin-shell ionosphere at 400 km.

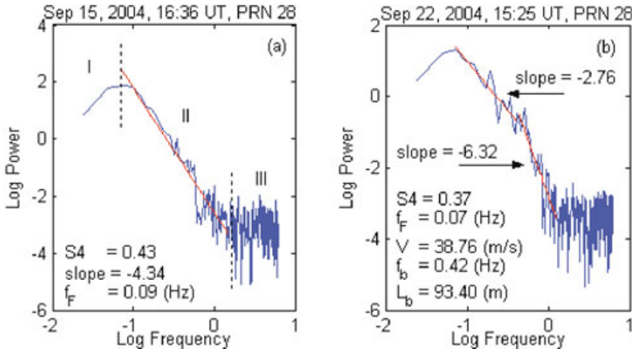

Fig. 1. (a) Power spectra of amplitude scintillation recorded at 1-min intervals at 16:36 UT on September 15, 2004. The Fresnel frequency and spectral slope are 0.09 Hz and −4.34, respectively during this period. (b) Power spectra of amplitude scintillation with a clear break in spectral slope recorded at 1-min intervals at 15:25 UT on Sep 22, 2004. The Fresnel frequency and break frequency are 0.07 and 0.42 Hz, respectively. The estimated zonal drift velocity is about 38.76 m/s and the scale length is about 93.40 m.

Since Sanya (18.33°N, 109.52°E) lies within the equatorial anomaly crest region, nighttime scintillations that are associated with F-region ionospheric irregularities are considered in this paper. Data from satellites with an elevation angle greater than 40° and with a time of lock greater than 180 s are taken into account. The data in the following several nights have been selected in our detailed analyses: (1) September 15, 2004, PRN 28; (2) September 22, 2004, PRN 04 and 28; (3) October 5, 2004, PRN 31.

3. Results and Discussion

We first consider the power spectral density of scintillation. According to Fig. 1(a), three main portions of scintillation power spectra can be explained. From left to right, we have the low frequency, the high frequency roll-off and the noise floor, respectively. Fresnel frequency (f_F) is the transition frequency between the low frequency and the high frequency roll-off part. Noise floor starting frequency is the transition frequency between the high frequency roll-off and the noise floor part. The high frequency roll-off part contains detailed information on ionospheric irregularities (Banerjee *et al.*, 1992). The spectral slope of this part is estimated from the linear high frequency roll-off portion of the log-log plot of power versus frequency by fitting a straight line to the steepest part using the least square technique. From Fig. 1(a), the spectral slope works out to be −4.34. The slope is related to the power spectral index (n) for the irregularities by

$$n = -(\text{slope}). \tag{1}$$

Fresnel frequency is estimated from the center of the broad maxima of about 0.09 Hz in Fig. 1(a).

The temporal power spectrum of radio waves scintillation is related to the in situ spatial spectrum of scintillation producing irregularities on the radio waves traversing through

the ionosphere. Briggs and Parkin (1963) proposed that the spectra of the electron density fluctuations along with the associated autocorrelation function obeyed generalized Gaussian statistics. However, Rufenach (1972) showed that a power law electron density fluctuation spectrum was more appropriate. Wernik *et al.* (1997) reported that the spectrum fits the power law quite well at high frequencies for weak scintillation and that spectrum appears to be Gaussian rather than a power law for moderately strong scintillation. Postulating the irregularities are Gaussian, the plot of Fourier Spectral Power in dB versus frequency squared should be a straight line above the Fresnel frequency (f_F). On the other hand, if irregularities have a power law spectrum, the plot of Fourier Spectral Power in dB versus log frequency should be a straight line for frequencies in excess of the Fresnel frequency (Singleton, 1974; Banola *et al.*, 2005). In our analyzed data set, the spectrum is always a power law spectrum.

On occasion, the spectrum is found with a clear break in spectral slope. Hysell *et al.* (1994) once showed that the wavelength at which the spectrum breaks is determined by the ambipolar diffusion coefficient. Figure 1(b) shows that the Fresnel break frequency (f_b) and Fresnel frequency (f_F) are approximately 0.42 and 0.07 Hz, respectively. In a situation where the eastward motion of the ionospheric pierce point (IPP) for a signal path nearly matches the eastward drift of the ionospheric irregularities, the irregularity drift velocity $\vec{V}$ relative to the signal path may be small enough to yield a Fresnel frequency smaller than 0.1 Hz (Bhattacharyya *et al.*, 2000). Consequently, the subtraction of the IPP motion can provide the actual information of the irregularity drift velocity. In general, the irregularity drift velocity is in a zonal direction, as has been reported by many authors, and as the trajectory of the GPS satellite is known, the actual zonal drift velocity of irregularities can be estimated by using the assumption that the irregularity drifts in only the zonal direction.

As $f_b = V/L_b$, we obtained the scale size (L_b) of ionospheric irregularity of about 93 m. Here, the zonal drift velocity (V) is estimated from

$$\vec{V} + \vec{V}_s = \vec{V}_f \tag{2}$$

where V_s is the IPP velocity, and V_f is the velocity estimated from the Fresnel frequency (f_F) (Yeh and Liu, 1982),

$$f_F = V_f/\sqrt{(2\lambda Z)}, \tag{3}$$

where λ is the signal wavelength, and Z is the effective distance between the receiver and the irregularities slab. Taking into consideration that the height of the ionospheric F2 layer varies through the night as well as from day to day and that the coherence scale depends on the height of the irregularity layer and the irregularity power spectral index for weak scintillation (Engavale and Bhattacharyya, 2005), we used the peak height of the F2-layer observed at Fuke (19.4°N, 109.0°E) by the DPS-4 ionosonde as the estimated height of the F-layer. Also taking into consideration the signal path elevation angle for different GPS satellite, we can estimate Z from the following equation,

$$Z = (R_E + H_r) \times \cos(\alpha) - R_E \times \sin(\beta) \tag{4}$$

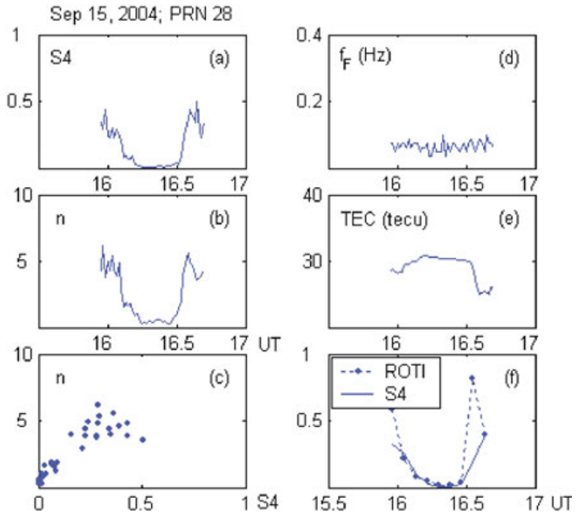

Fig. 2(I). Comparison of the amplitude scintillation index with the spectral index and total electron content observed from PRN 28 at Sanya on September 15, 2004. (a) Variation in the amplitude scintillation index (S4) at 1-min intervals. (b) Variation in the spectral index (n) at 1-min intervals. (c) Variation of n with S4. (d) Variation in the Fresnel frequency at 1-min intervals. (e) Variation in the total electron content (TEC) at 1-min intervals. (f) The standard deviation of rate of change of TEC at 5-min intervals (ROTI) and the mean of the S4 index at 5-min intervals.

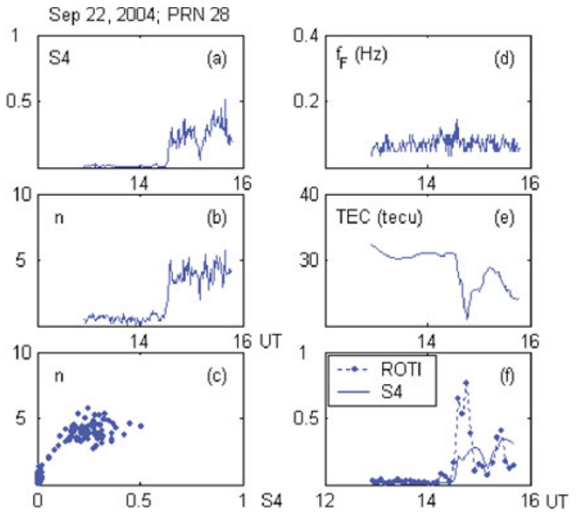

Fig. 2(II). As in Fig. 2(I) for PRN 28 on September 22, 2004.

$$\alpha = \arcsin((R_E/(R_E + H_r)) \times \cos(\beta)) \tag{5}$$

where R_E is the radius of the Earth, β is the elevation angle of GPS satellite, H_r and is the height of the irregularities; here, the height was measured at Fuke, as noted in the previous paragraph.

Figure 2(I) and 2(II) show the results of the analysis of data recorded from PRN 28 on September 15, 2004 and September 22, 2004, respectively. Panel (a) shows the UT variation in amplitude scintillation, while Panels (b) and (c) show the variation in the spectral index (n) with the UT and S4 index, respectively. The Fresnel frequency (f_F) is shown in Panel (d). By assuming the ionosphere to be a single-layer-model, the slant TEC value can be converted

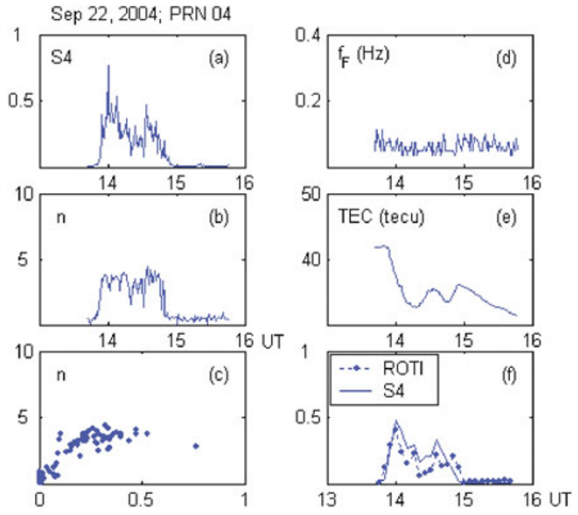

Fig. 3(I). As in Fig. 2(I) for PRN 4 on September 22, 2004. However, at most times ROTI is smaller than the fluctuation of S4, and the ratio ROTI/S4 is less than 1.

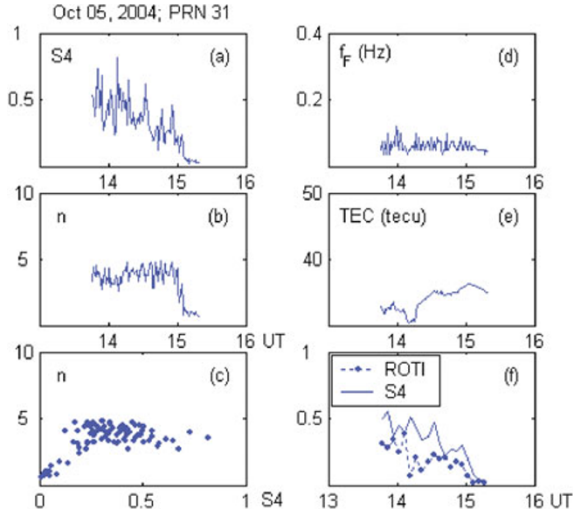

Fig. 3(II). As in Fig. 3(I) for PRN 31 on October 5, 2004.

to equivalent vertical TEC,

$$\mathrm{VTEC} = (\mathrm{STEC} + \mathrm{Bias}) \times \cos(\alpha) \tag{6}$$

where α is the incidence angle at the thin-shell ionosphere altitude of a ray from the GPS satellite to a ground receiver; replacing H_r with H_{sp}, it is same as defined in Eq. (5). H_{sp} is the height of the sub-ionosphere point and is assumed here to be 400 km. Bias is instrumental bias.

The variation in the equivalent vertical TEC with UT is shown in Panel (e). Since ROTI values are obtained at 5-min intervals, the S4 values, derived at 1-min intervals, have been averaged over 5-min intervals. Panel (f) illustrates the variation of ROTI and the mean of S4. A close comparison of Panels (a) and (b) shows that there is an increase in spectral indices (n) corresponding to the increase in amplitude scintillation activities. During the decay phase of amplitude scintillation, the spectral indices are also found to decrease whether pre-midnight or post-midnight. According to Panels (e) and (f), the presence of some large-scale depletions

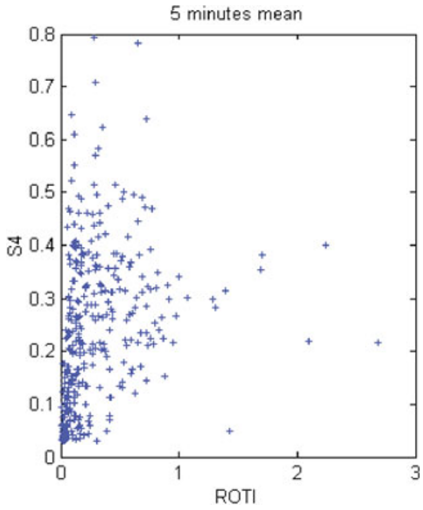

Fig. 4. A scatter plot of a 5-min mean of ROTI and S4 when all scintillation events are considered during the period July 2004–July 2005. The elevation angle was confined to greater than 40°.

of TEC or plasma bubbles may be noted during the pre-midnight to post-midnight hours (16:30–17:00 UT, 23:50–00:20 LT). TEC depletions in Panel (e) correspond to larger values of ROTI, and increased fluctuations of S4 are shown in Panel (f). These show that in the pre- and post-midnight periods, amplitude scintillations or plasma bubbles are detected with associated large-scale irregularities.

Figure 3(I) and 3(II) show a similar result: the trend of spectral indices (n) and ROTI correspond well with the trend of S4 indices during the generation, evolution, and decay phase of amplitude scintillation. The S4 indices and spectral indices do not show any clear relationship with Fresnel frequencies, but the range of variation in ROTI/S4 is different in Fig. 2(I, II). As shown in Fig. 2(I, II), when scintillation occurs, apparent TEC depletions exist. Hence, the ratio of ROTI/S4 is greater than 1. However, in Fig. 3(I, II), ROTI is mostly smaller than the fluctuation of the S4 index, leading to the ratio of ROTI/S4 being less than 1 since TEC is a line-integrated electron density along the satellite signal path, and S4 is the normalized root mean square deviation of signal power. In general, ROTI is more weighted towards large-scale depletion changes and the S4 index is weighted towards small-scale density fluctuations. When small-scale irregularities (scintillation) exist, large-scale plasma depletions do in fact exist. Here, the observed lower value of the ROTI/S4 ratio probably indicates that the variation of large-scale plasma depletion is not apparent.

Figure 4 shows a scatter plot of 5-min average values of S4 and ROTI. It indicates that when all satellites are considered and the scintillation occurs (S4 $\geq$ 0.1) during the period July 2004-July 2005, the ratio ROTI/S4 varies between 0.3 and 6. By using GPS TEC data obtained from the GPS receivers at Ascension Island (7.95°S, 14.45°W), Basu *et al.* (1999) found that ROTI/S4 varies between 2 and 10. The quantitative relationship between ROTI and S4 varies considerably due to variations in the ionospheric projection of the satellite velocity and the ionospheric irregularity drift. For different GPS satellites with varying satel-

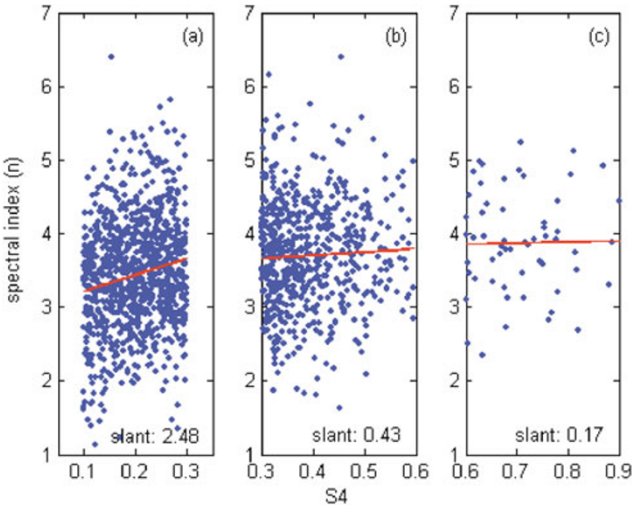

Fig. 5. Variation of the spectral index (n) with amplitude scintillation index (S4) when all scintillation events are considered during the period July 2004–July 2005. (a), (b) and (c) show the variation in the spectral index with weak, moderate and strong amplitude scintillation; the slant of the auto-regression line is 2.48, 0.43 and 0.17, respectively.

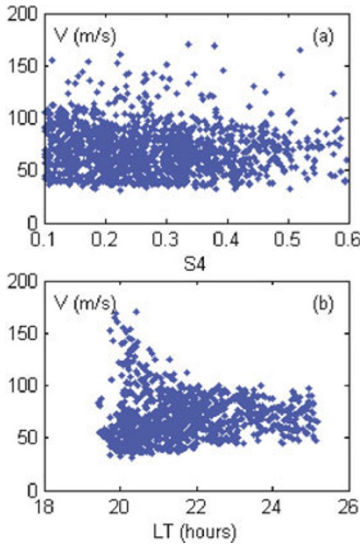

Fig. 6. (a) Variation of the zonal drift velocity (V) with the S4 index when all weak and moderate scintillations are considered. (b) Variation in the zonal drift velocity (V) observed at Sanya during geomagnetic quiet nights ($Kp < 3$) considering all weak and moderate scintillations.

lite trajectories, the ionospheric projection of the satellite velocity is different; even for the same irregularity drift, the scale length of ROTI for different satellites will be different. Hence, it is difficult to obtain quantitative estimates of scintillation from the analysis of ROTI. At high latitudes, the ionospheric motion during active conditions may approach speeds of a few kilometers per second. Therefore, the ratio of ROTI/S4 at high latitudes may be considerably larger than that in the equatorial region (Basu *et al.*, 1999).

In order to understand the relationship between the S4 index and the spectral index (n), a mass plot of the S4 index and spectral index is shown in Fig. 5. This plot indicates that when all scintillation activities are considered, the spectral index increases with increasing S4 index for weak amplitude scintillation ($0.1 \leq S4 < 0.3$) (Fig. 5, Panel (a)). However, for moderate and strong scintillation ($S4 \geq 0.3$), the spectral index is likely to be a constant value (Fig. 5, Panels (b) and (c)). The slant of the auto-regression line is 2.48, 0.43 and 0.17 respectively. The sub-panel c of Figs. 2(I, II) and 3(I, II) also show this characteristic. This probably means that the spectral index tends to be saturated when moderate and strong amplitude scintillation occurs.

At the high latitude station Aberystwyth (52.4°N, 4.1°W), Kersley and Chandra (1984) obtained a spectral index in the range 2.5–4.8, with average value of 3.58 for scintillation observed from radar and VHF scintillation measurements. They also reported an increase in the spectral index with increasing scintillation index S4. At a low latitude region, Fang and Liu (1984) also found an increase in the spectral index with increasing S4 for scintillations observed from the GHz band at Hong Kong (22.3°N, 114.2°E). These results can be explained on the basis that the S4 index depends on the phase fluctuation and the fluctuation is further determined by the density fluctuation and power spectral index. Therefore, when S4 is mainly determined by the power spectral index, an increase in n with an increase in the S4 index will be observed. The structuring and evolution of equatorial spread F (ESF) irregularities change from day-to-day and through the night, and they depend on background conditions; the power spectral characteristic of irregularity also changes over time. For a given time instant, the estimated S4 may derive from a different combination of density fluctuations and power spectral index. Engavale and Bhattacharyya (2005) reported that when phase fluctuations imposing on the radio signal are fixed, S4 decreases with increases in the power spectral index.

By analyzing approximately 100 scintillation events recorded at Ahmedabad (23.2°N, 72.4°E), Vyas and Chandra (1994) reported spectral indices in the range of 1.0 to 5.0, with a mean value of 2.8. Basu *et al.* (1980) reported higher values of spectral index at the anomaly crest location (Ascension Island, 7.95°S, 14.45°W) than at the equatorial location (Ancon (11.50°S, 77.10°W) and Huancayo (12.05°S, 75.12°W)), but they stated that the results were not conclusive. At the same time, using in situ data obtained from AE-E satellite, they obtained a spectral index value of 2.8 for scale sizes of less than 1 km, and 1.5 for scale sizes greater than 1 km. The spectral indices (n) of our present study are shown to be between 1.0 and 6.4, and the mean value is 3.6 for moderate and strong GPS ionospheric scintillations ($S4 \geq 0.3$); this probably corresponds to a scale size of meters to hundred meters. Ambient ionospheric conditions usually play important roles in the evolution and structuring of ionospheric irregularities, and these conditions vary from day to day and may be different at different locations. Hence, the differences in the structuring of ionospheric irregularities are probably related to the observed location and time period.

Figure 6(a) shows the zonal drift velocity of irregularities (V) with weak and moderate amplitude scintillation activities. As noted in the previous paragraph, the estimated velocity V_f from Fresnel frequency is the vector sum of the satellite motion and the irregularities in a direction perpen-

dicular to the propagation path. Since the geometry of the signal path in relation to the irregularities keeps changing in the course of a satellite's orbit, the situation is more complex than when a geostationary satellite is used. By using the assumption that the irregularity drifts in only a zonal direction, the actual zonal drift velocity of the irregularities has been estimated, as shown in Fig. 6(a) and (b). This figure shows that the velocity does not have any clear relation with the S4 index. We are planning to set up a second GPS ionospheric scintillation/TEC receiver at Sanya. The two receivers will be aligned along the east-west direction. In this way, the influence of the satellite motion can be eliminated during the analysis of scintillation spectrum.

Figure 6(b) shows a mass plot of the drift velocities (V) during geomagnetic quiet nights ($Kp < 3$) with LT for weak and moderate scintillation activities ($0.1 \leq$ S4 $<$ 0.6). It reveals a great deal of day-to-day variability in the velocity before 22:00 LT. After 22:00 LT, the velocities estimated on different days of the years fall into the same pattern. This plot may be considered to be representative of the ambient plasma drift. The results probably indicate that velocity structures associated with perturbation electric fields in the equatorial F-region are eroded in a couple of hours after the development of irregularities is initiated, while the density structures associated with scintillation-producing irregularities continue to exist for several hours longer (Bhattacharyya *et al*., 2001).

4. Summary

The spectral characteristics of irregularities and TEC fluctuations are studied using amplitude scintillation and TEC data recorded by a GPS ionospheric scintillation and TEC receiver at Sanya. An estimate of the zonal drift velocity of irregularities is also presented.

The main results can be summarized as follows. (1) When scintillation is considered to occur, the ratio ROTI/S4 varies between 0.3 and 6 in our data set (elevation angle was confined to greater than 40°). Small- and large-scale irregularities may coexist during the pre- and post-midnight period. Based on the assumptions that the ratio ROTI/S4 is due to the variations of the projected satellite velocity in the ionosphere and the irregularity drift, it is difficult to obtain quantitative estimates of scintillation from the analysis of ROTI. (2) The spectral index shows a linear change with a weak amplitude scintillation index ($0.1 \leq$ S4 < 0.3). It increases towards the generation phase of amplitude scintillation activities and decreases toward the decay phase. However, for moderate and strong amplitude scintillation (S4 ≥ 0.3), the spectral index tends to be saturated. The spectral indices range from 1.0 to 6.4, with a mean value of 3.6. (3) There is no evident correspondence between the Fresnel frequency, the spectral index, and the amplitude scintillation index during these scintillation events. The correlation between drift velocity and LT probably demonstrates that the motion of the irregularities which cause scintillations is highly variable in the initial phase of irregularity development on geomagnetic quiet days. After about 22:00 LT, the estimated velocity tends to follow the same pattern on different days. This resembles the results of Bhattacharyya *et al*. (2001) observed at Ancon. (4) We should note that the previous results on drift velocity are based on the assumption of the irregularity drifts in only the zonal direction. The space-aligned GPS receivers are necessary to eliminate the influence of satellite velocity and provide actual information on the irregularity drifts.

Acknowledgments. This research was supported by the National Natural Science Foundation of China (40574072, 40374054) and the KIP Pilot Project (KZCX3-SW-144) of Chinese Academy of Sciences. The authors also thank Prof. Jiankui Shi who provided the Fuke ionosonde data. Two anonymous reviewers are gratefully acknowledged for their suggestions on improving the manuscript.

References

Aarons, J., Global morphology of ionospheric scintillation, *Proc. IEEE*, **70**, 360–378, 1982.

Aarons, J., The longitudinal morphology of equatorial F-layer irregularities relevant to their occurrence, *Space Sci. Rev.*, **63**, 209–243, 1993.

Aarons, J., M. Mendillo, R. Yantosca, and E. Kudeki, GPS phase fluctuations in the equatorial region during the MISETA 1994 campaign, *J. Geophys. Res.*, **101**(A12), 26,851–26,862, 1996.

Aarons, J., M. Mendillo, and R. Yantosca, GPS phase fluctuations in the equatorial region during sunspot minimum, *Radio Sci.*, **32**(4), 1535–1550, 1997.

Basu, S. and B. K. Khan, Model of equatorial Scintillation from in-situ Measurements, *Radio Sci.*, **11**, 821–832, 1976.

Basu, S., S. Basu, J. Aarons, J. P. McClure, and M. D. Cousins, On the coexistence of kilometer- and meter-scale irregularities in the nighttime equatorial F-region, *J. Geophys. Res.*, **83**, 4219, 1978.

Basu, S., J. P. McClure, S. Basu, W. B. Hanson, and J. Aarons, Coordinated study of equatorial scintillation and in situ and radio observations of nighttime F region irregularities, *J. Geophys. Res.*, **85**, 5119–5130, 1980.

Basu, S. and S. Basu, Equatorial scintillations: Advances since ISEA-6, *J. Atmos. Terr. Phys.*, **47**, 753–768, 1985.

Basu, S. and S. Basu, Ionospheric structures and scintillation spectra, in *Wave Propagation in Random Media (Scintillation)*, edited by V. I. Tatarski, A. Ishimaru, and V. U. Zavorotny, 139–153, The International Society for Optical Engineering, Bellingham, WA, USA, 1993.

Basu, S., K. M. Groves, J. M. Quinn, and P. Doherty, A comparison of TEC fluctuations and scintillations at Ascension Island, *J. Atmos. Terr. Phys.*, **61**, 1219–1226, 1999.

Banerjee, P. K., R. S. Dabas, and B. M. Reddy, C and L band transionospheric scintillation experiment: some results for applications to Satellite Radio Systems, *Radio Sci.*, **27**(6), 955–969, 1992.

Banola, S., B. M. Pathan, D. R. K. Rao, and H. Chandra, Spectral characteristics of scintillations producing ionospheric irregularities in the Indian region, *Earth Planets Space*, **57**, 47–59, 2005.

Beach, T. L. and P. M. Kintner, Simultaneous Global Positioning System observations of equatorial scintillations and total electron content fluctuations, *J. Geophys. Res.*, **104**(A10), 22,553–22,566, 1999.

Bhattacharyya, A. and R. G. Rastogi, Amplitude scintillation during early and late phases of evolution of irregularities in the nighttime equatorial ionosphere, *Radio Sci.*, **20**(4), 935–946, 1985.

Bhattacharyya, A., R. G. Rastogi, and K. C. Yeh, Signal frequency dependence of ionospheric amplitude scintillation, *Radio Sci.*, **25**, 289–297, 1990.

Bhattacharyya, A. and R. G. Rastogi, structure of ionospheric irregularities from amplitude and phase scintillation observations, *Radio Sci.*, **26**(2), 439–449, 1991.

Bhattacharyya, A., K. C. Yeh, and S. J. Franke, Deducing turbulence parameters from transionospheric scintillation measurements, *Space Sci. Rev.*, **61**, 335–386, 1992.

Bhattacharyya, A., T. L. Beach, S. Baus, and P. M. Kintner, Nighttime equatorial ionosphere: GPS scintillations and differential carrier phase fluctuations, *Radio Sci.*, **35**(1), 209–224, 2000.

Bhattacharyya, A., S. Basu, K. M. Groves, C. E. Valladares, and R. Sheehan, Dynamics of equatorial F region irregularities from spaced receiver scintillation observations, *Geophys. Res. Lett.*, **28**(1), 119–122, 2001.

Bhattacharyya, A., K. M. Groves, S. Basu, H. Kuenzler, C. Valladares, and R. Sheehan, L-band scintillation activity and space-time structure of low-latitude UHF scintillations, *Radio Sci.*, **38**(1), 1004–1013, 2003.

Briggs, B. H. and I. A. Parkin, On the variation of radio star and satellite

scintillations with zenith angle, *J. Atmos. Terr. Phys.*, **25**, 339–366, 1963.

Chandra, H., Hari Om Vats, G. Sethia, M. R. Deshpande, R. G. Rastogi, J. H. Sastri, and B. S. Murthy, Ionospheric scintillations associated with features of equatorial ionosphere, *Ann. Geophys.*, **35**, 145–151, 1979.

Engavale, B. and A. Bhattacharyya, Spatial correlation function of intensity variations in the ground scintillation pattern produced by equatorial spread-F irregularities, *Indian J. Radio Space Phys.*, **34**(1), 22–32, 2005.

Fang, D. J. and C. H. Liu, Statistical characterizations of equatorial scintillation in the Asia region, *Radio Sci.*, **19**, 345–358, 1984.

Fejer, B. G., Natural ionospheric plasma waves, in *Modern Ionospheric Science*, edited by H. Kohl, R. Ruster, and K. Schlegel, 216–273, European Geophysical Society, Katlenburg-Lindau, FRG, 1996.

Haerendal, G., Report, Max Planck Institue fur physik und Astrophysik, Garching, West Germany, 1973.

Heppner, J. P., M. C. Liebrecht, N. C. Maynard, and R. F. Pfaff, High-latitude distributions of plasma waves and spatial irregularities from DE2 alternating current electric field observations, *J. Geophys. Res.*, **98**, 1629–1652, 1993.

Hysell, D. L., M. C. Kelley, W. E. Swartz, R. F. Pfaff, and C. M. Swenson, Steepened structures in equatorial spread F, 2. Theory, *J. Geophys. Res.*, **99**, 8841–8850, 1994.

Kersley, L. and H. Chandra, Power spectra of VHF intensity scintillations from F2 and E region ionospheric irregularities, *J. Atmos. Terr. Phys.*, **46**(8), 667–672, 1984.

Keskinen, M. J. and S. L. Ossakow, Theories of high-latitude irregularities: A review, *Radio Sci.*, **18**, 1077–1092, 1983.

Li, G., B. Ning, and H. Yuan, Design and realization of a real-time GPS ionospheric scintillation monitoring system, *Chinese Journal of Radio Science*, **20**(6), 758–765, 2005.

Pathan, B. M., P. V. Koparkar, R. G. Rastogi, and D. R. K. Rao, Dynamics of ionospheric irregularities producing VHF radio wave scintillations at low latitudes, *Annu. Geophys.*, **9**, 126–132, 1991.

Pi, X., A. J. Mannucci, U. J. Lindqwister, and C. M. Ho, Monitoring of global ionospheric irregularities using the worldwide GPS network, *Geophys. Res. Lett.*, **24**, 2283, 1997.

Rastogi, R. G., Solar cycle effect in radio wave scintillations at Huancayo, *Ind. J. Radio Space Phys.*, **11**, 215–221, 1982.

Rastogi, R. G., H. Chandra, and M. R. Deshpande, Equatorial radio scintillations of ATS-6 radio beacons: Phase II Ootacamund 1975–76, *Ind. J. Radio Space Phys.*, **11**, 240–246, 1982.

Rufenach, C. L., Power law wavenumber spectrum deduced from ionospheric scintillation observations, *J. Geophys. Res.*, **77**, 4761–4772, 1972.

Singleton, D. G., Power spectra of ionospheric scintillations, *J. Atmos. Terr. Phys.*, **36**, 113–133, 1974.

Taur, R. R., Ionospheric scintillations at 4 to 6 GHz, *COMSAT Tech. Rev.*, **3**, 145–163, 1973.

Van Dierendonck, A. J., Q. Hua, and J. Klobuchar, Ionospheric scintillation monitoring using commercial single frequency C/A code receivers, Proceedings of ION GPS 93, Salt Lake City, UT, 22–24 September, 1333–1342, 1993.

Vyas, G. D. and H. Chandra, VHF scintillation and spread-F in the anomaly crest region, *Ind. J. Radio Space Phys.*, **23**, 157–164, 1994.

Wernik, A. W., Wavelet transform of nonstationary ionospheric scintillation, *Acta Geophys. Polonica*, **45**, 237–253, 1997.

Woodman, R. F. and C. LaHoz, Radar observations of F-region equatorial irregularities, *J. Geophys. Res.*, **81**, 5447–5461, 1976.

Yeh, K. C. and C. H. Liu, Radio-wave scintillations in the ionosphere, *Proc. IEEE*, **70**, 324–360, 1982.

G. Li, B. Ning (nbq@mail.iggcas.ac.cn), and H. Yuan